

## STOP PRODUCTION AT HADRON COLLIDERS

W. BEENAKKER<sup>1§</sup>, M. KRÄMER<sup>2</sup>, T. PLEHN<sup>3</sup>, M. SPIRA<sup>4</sup>, AND P.M. ZERWAS<sup>3</sup><sup>1</sup> Instituut–Lorentz, University of Leiden, The Netherlands<sup>2</sup> Rutherford Appleton Laboratory, Chilton, Didcot, OX11 0QX, UK<sup>3</sup> Deutsches Elektronen–Synchrotron DESY, D–22603 Hamburg, FRG<sup>4</sup> CERN, Theory Division, CH–1211 Geneva 23, Switzerland**Abstract**

Stop particles are expected to be the lightest squarks in supersymmetric theories and the search for these particles is an important experimental task. We therefore present the cross sections for the production processes  $p\bar{p}/pp \rightarrow \tilde{t}_1\bar{\tilde{t}}_1$  and  $\tilde{t}_2\bar{\tilde{t}}_2$  at Tevatron and LHC energies in next-to-leading order supersymmetric QCD. The corrections stabilize the theoretical predictions for the cross sections, and they are positive, thus raising the cross sections to values above the leading-order predictions. Mixed  $\tilde{t}_1\bar{\tilde{t}}_2/\bar{\tilde{t}}_1\tilde{t}_2$  pairs can only be generated in higher orders at strongly suppressed rates.

---

<sup>§</sup>Research supported by a fellowship of the Royal Dutch Academy of Arts and Sciences.

# 1 Introduction

Within the squark sector of supersymmetric theories, the top-squark (stop) eigenstate  $\tilde{t}_1$  is expected to be the lightest particle [1]. If the scalar masses in grand unified theories, for instance, are evolved from universal values at the GUT scale down to low scales the  $\tilde{t}_1$  top-squark drops to the lowest value in the squark spectrum. Moreover, the strong Yukawa coupling between top/stop and Higgs fields gives rise to large mixing, leading to a potentially small mass eigenvalue for  $\tilde{t}_1$  [2].

In  $e^+e^-$  and  $p\bar{p}/pp$  collisions stop particles are produced in pairs. Present limits from LEP2 indicate a  $\tilde{t}_1$  mass in excess of 67 GeV, independent of the mixing angle in the stop sector, but depending on the lightest neutralino mass [3]. Preliminary analyses at the Tevatron have led to a lower limit of 93 GeV for the  $\tilde{t}_1$  mass, depending on the lightest neutralino mass [4].

The cross sections for the production of squarks ( $\tilde{q}$ ) and gluinos ( $\tilde{g}$ ) in hadron collisions have been calculated at the Born level already quite some time ago [5]. Only recently have these theoretical predictions been improved by calculations of the next-to-leading order (NLO) SUSY-QCD corrections for squark/gluino production, with the final-state squarks restricted to the light-flavor sector ( $\tilde{q} \neq \tilde{t}$ ) [6]. In the present paper we supplement this analysis by the corresponding analysis for the stop sector

$$p\bar{p}/pp \rightarrow \tilde{t}_1\bar{\tilde{t}}_1 + X \quad \text{and} \quad \tilde{t}_2\bar{\tilde{t}}_2 + X \quad (1)$$

in the  $p\bar{p}$  collisions of the Tevatron and the  $pp$  collisions of the LHC. This NLO calculation is motivated by two requirements: First, to stabilize the theoretical predictions for the cross sections with respect to the renormalization and factorization scales, which introduce spurious parameters into fixed-order calculations. And second, to improve the accuracy of the theoretical predictions for the cross sections. Extending the light-flavor analysis to stop production is a necessary step since the mixing effects must be taken into account properly. At NLO [*i.e.*  $\mathcal{O}(\alpha_s^3)$ ] the production cross sections are still diagonal in the stop sector. The production of mixed  $\tilde{t}_1\bar{\tilde{t}}_2/\tilde{t}_2\bar{\tilde{t}}_1$  pairs is suppressed as the cross section is of order  $\alpha_s^4$ . Since the calculation is rather involved but the rate is small, we have studied this process in the limit of large gluino mass to exemplify the expected size of the non-diagonal cross section.

The cross sections for the diagonal production of stop particles, Eq. (1), depend essentially only on the mass of the produced stop particles,  $m_{\tilde{t}_1}$  or  $m_{\tilde{t}_2}$ . The dependence of the cross sections on the other SUSY parameters, *i.e.* the gluino mass  $m_{\tilde{g}}$ , the masses of the other squarks and the mixing angle  $\tilde{\theta}$ , is very weak since these parameters affect only the higher-order corrections and are not relevant at leading order.

The results for the diagonal production of stop particles,  $\tilde{t}_1\bar{\tilde{t}}_1$  and  $\tilde{t}_2\bar{\tilde{t}}_2$ , will be discussed in the next section. The size of the cross section for mixed-pair production  $\tilde{t}_1\bar{\tilde{t}}_2$  and  $\tilde{t}_2\bar{\tilde{t}}_1$  will be estimated subsequently.

## 2 Diagonal stop-pair production

At hadron colliders, diagonal pairs of stop particles can be produced at lowest order QCD in quark–antiquark annihilation and gluon–gluon fusion:

$$\begin{aligned} q\bar{q} &\rightarrow \tilde{t}_1\bar{\tilde{t}}_1 \quad \text{and} \quad \tilde{t}_2\bar{\tilde{t}}_2 \\ gg &\rightarrow \tilde{t}_1\bar{\tilde{t}}_1 \quad \text{and} \quad \tilde{t}_2\bar{\tilde{t}}_2 \end{aligned} \quad (2)$$

Mixed pairs  $\tilde{t}_1\bar{\tilde{t}}_2$  and  $\tilde{t}_2\bar{\tilde{t}}_1$  cannot be produced in lowest order since the  $g\tilde{t}\tilde{t}$  and  $gg\tilde{t}\tilde{t}$  vertices are diagonal in the chiral as well as in the mass basis. The relevant diagrams for the reactions (2) are shown in Fig. 1a. The corresponding cross sections for these partonic subprocesses may be written as ( $k = 1, 2$ ):

$$\hat{\sigma}_{LO}[q\bar{q} \rightarrow \tilde{t}_k\bar{\tilde{t}}_k] = \frac{\alpha_s^2\pi}{s} \frac{2}{27} \beta_k^3 \quad (3)$$

$$\hat{\sigma}_{LO}[gg \rightarrow \tilde{t}_k\bar{\tilde{t}}_k] = \frac{\alpha_s^2\pi}{s} \left\{ \beta_k \left( \frac{5}{48} + \frac{31m_{\tilde{t}_k}^2}{24s} \right) + \left( \frac{2m_{\tilde{t}_k}^2}{3s} + \frac{m_{\tilde{t}_k}^4}{6s^2} \right) \log \left( \frac{1 - \beta_k}{1 + \beta_k} \right) \right\} \quad (4)$$

The invariant energy of the subprocess is denoted by  $\sqrt{s}$ , the velocity by  $\beta_k = \sqrt{1 - 4m_{\tilde{t}_k}^2/s}$ . The cross sections coincide with the corresponding expressions for light-flavor squarks in the limit of large gluino masses, cf. Ref. [6].

The hadronic  $p\bar{p}/pp$  cross sections are obtained by folding the partonic cross sections with the  $q\bar{q}$  and  $gg$  luminosities. At the Tevatron the dominant mechanism for large stop masses is the valence  $q\bar{q}$  annihilation. The fraction of  $q\bar{q}$  events rises from 0.55 to 0.86, if the  $\tilde{t}_1$  mass is increased from 100 to 200 GeV. At the LHC the gluon-fusion mechanism plays a more prominent role. For a  $\tilde{t}_1$  mass below 200 GeV, more than 90% of the events are generated by  $gg$  fusion, cf. Table 1.

We closely follow the approach of Ref. [6] for the calculation of the NLO SUSY-QCD corrections. The virtual  $\mathcal{O}(\alpha_s)$  corrections involve the usual SUSY-QCD corrections to the propagators and vertices, as well as box and rescattering diagrams, cf. Ref. [6]. To this order the mixing angle  $\tilde{\theta}$  enters the cross section only through corrections involving the  $t\tilde{t}\tilde{g}$  and the four-squark couplings. The relevant couplings of this type are described by the Lagrangeans

$$\begin{aligned} \mathcal{L}_3 &= -\sqrt{2}g_s T_{ij}^a (1 + \mathcal{P}_{12}) \bar{\tilde{g}}_a \left[ \cos\tilde{\theta} \frac{1}{2}(1 - \gamma_5) - \sin\tilde{\theta} \frac{1}{2}(1 + \gamma_5) \right] t_j \tilde{t}_{1i}^* + \text{h.c.} \\ \mathcal{L}_4 &= -\frac{g_s^2}{8} (1 + \mathcal{P}_{12}) \tilde{t}_{1i}^* \tilde{t}_{1j} \left\{ \cos^2(2\tilde{\theta}) A_2^{ijkl} \tilde{t}_{1k}^* \tilde{t}_{1l} + 2 \left[ \sin^2(2\tilde{\theta}) A_2^{ijkl} - A_1^{ijkl} \right] \tilde{t}_{2k}^* \tilde{t}_{2l} \right. \\ &\quad \left. + 4 \cos(2\tilde{\theta}) A_1^{ijkl} \sum_{\tilde{q} \neq \tilde{t}} (\tilde{q}_{Lk}^* \tilde{q}_{Ll} - \tilde{q}_{Rk}^* \tilde{q}_{Rl}) \right\} \end{aligned} \quad (5)$$

with the color tensors ( $N_c=3$ )

$$\begin{aligned} A_1^{ijkl} &= \delta^{il} \delta^{kj} - \delta^{ij} \delta^{kl} / N_c \\ A_2^{ijkl} &= \left( \delta^{il} \delta^{kj} + \delta^{ij} \delta^{kl} \right) (N_c - 1) / N_c \end{aligned} \quad (6)$$

Here  $\tilde{q}_{L/R}$  represent the left(L)- and right(R)-chirality light-flavor squarks. Indices of the fundamental/adjoint representation of color  $SU(3)$  are denoted by  $i, j, k$  and  $a$ , respectively, and the generators of the fundamental representation by  $T^a$ . The operator  $\mathcal{P}_{12}$  permutes the 1- and 2-components of the top-squarks:

$$\mathcal{P}_{12} \quad : \quad [\tilde{t}_1 \leftrightarrow \tilde{t}_2; \cos \tilde{\theta} \rightarrow -\sin \tilde{\theta}, \sin \tilde{\theta} \rightarrow \cos \tilde{\theta}] \quad (7)$$

Two typical diagrams in which  $\tilde{\theta}$  enters the scattering amplitude  $gg \rightarrow \tilde{t}_k \bar{\tilde{t}}_k$  through vertex and rescattering corrections are shown in Fig. 1b. Since mixing enters explicitly only through higher-order diagrams, the angle  $\tilde{\theta}$  need not be renormalized [7] in the present calculation and it can be identified with the lowest-order expression derived from the stop mass matrix.

As usual, the virtual corrections are supplemented by gluon radiation from color lines and vertices, as well as contributions from the inelastic Compton processes  $gg \rightarrow \tilde{t}_k \bar{\tilde{t}}_k q$  and  $g\bar{q} \rightarrow \tilde{t}_k \bar{\tilde{t}}_k \bar{q}$ , cf. Ref.[6] for diagrammatic details.

The singularities associated with the NLO corrections are isolated by means of dimensional regularization and renormalized within the  $\overline{\text{MS}}$  scheme.<sup>1</sup> The renormalization of the QCD coupling is performed in such a way that the heavy particles (top quarks, gluinos, and light-flavor squarks) are decoupled smoothly for momenta smaller than their masses. This implies that the heavy particles do not contribute to the evolution of the couplings and parton densities. The masses of the light quarks ( $q \neq t$ ) are neglected and the top-quark mass is set to  $m_t = 175$  GeV. For the calculation of gluon bremsstrahlung, the phase space for gluon radiation is split into two distinct regimes, one accounting for soft gluons and the other for the hard gluons. The separation is implemented by introducing a cut-off parameter  $\Delta$  in the invariant mass of the radiated gluon and one of the heavy particles in the final state. The cut-off parameter is chosen so small that it can be neglected with respect to any other mass scale in the process. As a result of the split-up of the phase space, terms of the form  $\log^i \Delta$  ( $i = 1, 2$ ) occur in both the soft and the hard cross sections. If soft and hard contributions are added up, any  $\Delta$  dependence disappears from the cross sections in the limit  $\Delta \rightarrow 0$ .

At lowest order, the cross sections for diagonal  $\tilde{t}_1 \bar{\tilde{t}}_1$  and  $\tilde{t}_2 \bar{\tilde{t}}_2$  pair production are given by the same analytical expression. At next-to-leading order, the  $t\bar{t}\tilde{g}$  and four-squark interactions will affect the production cross sections for the two diagonal pairs in different ways, introducing the explicit dependence on the mixing angle. However, the  $\tilde{\theta}$  dependence will turn out to be very mild. It follows from Eqs. (5), that the analysis of  $\tilde{t}_2 \bar{\tilde{t}}_2$  pairs can be copied from the analysis of  $\tilde{t}_1 \bar{\tilde{t}}_1$  pairs after applying the permutation  $\mathcal{P}_{12}$  defined in Eq. (7).

For the detailed description of the partonic cross-sections we introduce scaling functions  $f$ ,

$$\hat{\sigma}_{ij} = \frac{\alpha_s^2(\mu^2)}{m_{\tilde{t}_k}^2} \left\{ f_{ij}^B(\eta) + 4\pi\alpha_s(\mu^2) \left[ f_{ij}^{V+S}(\eta, r, \tilde{\theta}) + f_{ij}^H(\eta) + \bar{f}_{ij}(\eta) \log \left( \frac{\mu^2}{m_{\tilde{t}_k}^2} \right) \right] \right\} \quad (8)$$

with  $r$  generically denoting all possible mass ratios  $m/m_{\tilde{t}_k}$ . The indices  $i, j = g, q, \bar{q}$  indicate the partonic initial state of the reaction  $ij \rightarrow \tilde{t}_k \bar{\tilde{t}}_k$ . The center-of-mass energy of the partonic

---

<sup>1</sup>Note that the spurious breaking of supersymmetry in the  $\overline{\text{MS}}$  scheme [8] has no effect on the NLO stop-pair cross sections. The Yukawa couplings become effective only as a part of the higher-order corrections and need not be renormalized.

reaction,  $\sqrt{s}$ , is absorbed in the quantity  $\eta = s/4m_{t_k}^2 - 1$ , which is better suited for analyzing the scaling functions in the various regions of interest. We have identified the renormalization and factorization scales:  $\mu_R = \mu_F = \mu$ . The scaling functions are divided into the Born term  $f^B$ , the sum of virtual and soft-gluon corrections  $f^{V+S}$ , the hard-gluon corrections  $f^H$ , and the scale-dependent contributions  $\bar{f}$ . The  $\log^i \Delta$  ( $i = 1, 2$ ) terms are separated from the soft-gluon corrections and added to the hard-gluon part. The hard-gluon corrections are therefore independent of the cut-off for  $\Delta \rightarrow 0$ .

The scaling functions are displayed in Fig.2 for the quark–antiquark, gluon–gluon, and (anti)quark–gluon channels. The mixing angle and the gluino and light-flavor squark masses are defined in a minimal supergravity scenario that will be discussed later in detail. The dependence on these parameters is weak. In particular if the mixing angle is varied over the full range, the impact on  $f^{V+S}$ , the only scaling function affected by  $\theta$ , is very small. Due to the  $\beta^3$  behavior of the LO quark–antiquark cross section, not much structure is observed in this channel in the vicinity of the production threshold ( $\beta, \eta \ll 1$ ). However, for the gluon–gluon channel two sources of large corrections can be identified in the threshold region. First, the exchange of (long-range) Coulomb gluons between the slowly moving massive particles in the final state leads to a singular Sommerfeld correction  $\sim \pi\alpha_s/\beta$ , which compensates the LO phase-space suppression  $\beta$ . The scaling function  $f_{gg}^{V+S}$  therefore approaches a non-zero value at the threshold. [For the  $q\bar{q}$  incoming state the cross section remains suppressed  $\sim \beta^2$ , since the LO gluino-exchange contribution that dominates the threshold behavior of light-flavor squark-pair production [6], is absent for stop-pair production]. It should be noted, however, that the screening due to the non-zero lifetimes of the top-squarks reduces the Coulomb effect considerably. Second, as a result of the strong energy dependence of the gluon–gluon cross sections near threshold, large gluonic initial-state corrections of the type  $\beta \log^i \beta$  ( $i = 1, 2$ ) emerge. The leading  $\log^2 \beta$  terms are universal and can be exponentiated. Near threshold, the scaling functions can be expanded in  $\beta$ :

$$\begin{aligned}
f_{gg}^B &= \frac{7\pi\beta}{384} & f_{q\bar{q}}^B &= \frac{\pi\beta^3}{54} \\
f_{gg}^{V+S} &= f_{gg}^B \frac{11}{336\beta} & f_{q\bar{q}}^{V+S} &= -f_{q\bar{q}}^B \frac{1}{48\beta} \\
f_{gg}^H &= f_{gg}^B \left[ \frac{3}{2\pi^2} \log^2(8\beta^2) - \frac{183}{28\pi^2} \log(8\beta^2) \right] & f_{q\bar{q}}^H &= f_{q\bar{q}}^B \left[ \frac{2}{3\pi^2} \log^2(8\beta^2) - \frac{107}{36\pi^2} \log(8\beta^2) \right] \\
\bar{f}_{gg} &= -f_{gg}^B \frac{3}{2\pi^2} \log(8\beta^2) & \bar{f}_{q\bar{q}} &= -f_{q\bar{q}}^B \frac{2}{3\pi^2} \log(8\beta^2)
\end{aligned} \tag{9}$$

At high energies the NLO partonic cross sections in the gluon–gluon and (anti)quark–gluon channels approach non-zero limits asymptotically, to be contrasted with the scaling behavior  $\sim 1/s$  of the LO cross sections. This is caused by the nearly on-shell exchange of space-like gluons, associated with the inelastic Compton processes and gluon radiation in the fusion process. Exploiting the factorization in transverse gluon momentum at high energies, the high-energy scaling functions can be determined analytically:

$$\begin{aligned}
f_{gg}^H &= \frac{2159}{43200\pi} & f_{qg}^H &= \frac{2159}{194400\pi} \\
\bar{f}_{gg} &= -\frac{11}{720\pi} & \bar{f}_{qg} &= -\frac{11}{3240\pi}
\end{aligned} \tag{10}$$

The scaling functions  $f_{g\bar{q}}$  are identical to  $f_{qg}$ . The ratio of the  $f_{gg}$  and  $f_{qg}$  scaling functions is given by 9 : 2, corresponding to the probability for emitting a soft gluon from a gluon (twice) or a quark.

The numerical analyses of the hadronic cross sections have been performed for the Fermilab Tevatron  $p\bar{p}$  collider with a center-of-mass energy of  $\sqrt{S} = 1.8$  TeV, and for the CERN Large Hadron Collider (LHC) with a  $pp$  center-of-mass energy of  $\sqrt{S} = 14$  TeV. We have adopted the CTEQ4M parametrization of the parton densities [9]. The uncertainty due to different parametrizations of the parton densities in NLO is less than  $\sim 5\%$  at the Tevatron and less than  $\sim 10\%$  at the LHC (irrespective of the choice for the scale  $\mu$ ). The difference between the two estimates can be attributed to the fact that the experimentally well-determined valence quarks dominate at the Tevatron, while the gluons are more prominent at the LHC.

In Fig. 3 we present the dependence of the total cross sections for  $\tilde{t}_1\tilde{t}_1$  production on the renormalization and factorization scale  $\mu = \mu_R = \mu_F$ . For a consistent comparison of the LO and NLO results, we have calculated all quantities [ $\alpha_s(\mu_R^2)$ , the parton densities, and the partonic cross sections] in LO and NLO, respectively. In LO the scale dependence is steep and monotonic: changing the scale from  $\mu = 2m_{\tilde{t}_1}$  to  $\mu = m_{\tilde{t}_1}/2$ , the LO cross section increases by more than 100%. In NLO the scale dependence is strongly reduced, to about 30% in this interval at the Tevatron. At the same time the cross section is considerably enhanced at the central scale ( $\mu = m_{\tilde{t}_1}$ ). The results are qualitatively similar for the LHC.

The magnitude of the SUSY-QCD corrections is illustrated by the  $K$  factors in Table 1 for Tevatron and LHC energies. The  $K$  factor is defined as  $K = \sigma_{NLO}/\sigma_{LO}$ , with all quantities calculated consistently in lowest and in next-to-leading order. In these calculations the scale is fixed at the central value ( $\mu = m_{\tilde{t}_k}$ ). For illustration, the supersymmetric parameters have been fixed within the minimal supergravity (SUGRA) model<sup>2</sup> such that  $m_{\tilde{g}} = 284$  (627) GeV and  $\sin(2\tilde{\theta}) = -0.99$  ( $-0.94$ ) for the Tevatron and the LHC, respectively. The stop masses in these scenarios are given by  $m_{\tilde{t}_1} = 153$  (325) GeV and  $m_{\tilde{t}_2} = 347$  (592) GeV, all other squarks are assumed to be mass degenerate with  $m_{\tilde{q}} = 256$  (539) GeV. However, in order to focus on the mass dependence of the cross sections and of the NLO corrections, the mass of the produced stop particles is varied around the SUGRA-inspired central value, independently of the other SUSY parameters. In the mass range considered, the SUSY-QCD corrections are small (and negative) if the  $q\bar{q}$  initial state dominates, cf. Table 1. If, in contrast, the  $gg$  initial state dominates, the corrections are positive and reach a level of 30–40%. The relatively large mass dependence of the  $K$  factors for  $\tilde{t}_1\tilde{t}_1$  production at the Tevatron can therefore be attributed to the fact that the  $gg$  initial state is important for small  $m_{\tilde{t}_1}$ , whereas the  $q\bar{q}$  initial state dominates for large  $m_{\tilde{t}_1}$ .

The total cross sections play a crucial role in the experimental analyses. They either serve to extract the exclusion limits for the mass parameters from the data, or, in the case of discovery, they can be exploited to determine the masses of the stop particles. The total cross sections for  $p\bar{p}/pp \rightarrow \tilde{t}_1\tilde{t}_1, \tilde{t}_2\tilde{t}_2$  are given in Figs. 4/5 for the Tevatron/LHC, respectively. The cross sections depend essentially only on the masses of the produced stop particles, and very little on the other

---

<sup>2</sup>For an approximate solution of the renormalization-group equations in the SUGRA-inspired model, the program SPYTHIA [10] has been adopted. For the Tevatron (LHC) parameters the input values  $m_0 = 100$  GeV,  $m_{1/2} = 100$  (250) GeV,  $A_0 = 300$  GeV,  $\tan\beta = 1.75$ , and  $\mu > 0$  have been chosen, generating the mass and mixing parameters quoted above.

| $m_{\tilde{t}}$ [GeV]          | $K_{\text{Tevatron}}$ | $gg_{\text{in}} : q\bar{q}_{\text{in}}$ | $K_{\text{LHC}}$ | $gg_{\text{in}} : q\bar{q}_{\text{in}}$ |             |
|--------------------------------|-----------------------|---|------------------|---|-------------|
| $\tilde{t}_1\bar{\tilde{t}}_1$ | 70                    | 1.41                                    | 0.64 : 0.36      | 1.25                                    | 0.96 : 0.04 |
|                                | 110                   | 1.30                                    | 0.41 : 0.59      | 1.32                                    | 0.95 : 0.05 |
|                                | 150                   | 1.19                                    | 0.25 : 0.75      | 1.37                                    | 0.94 : 0.06 |
|                                | 190                   | 1.11                                    | 0.15 : 0.85      | 1.40                                    | 0.92 : 0.08 |
| $\tilde{t}_2\bar{\tilde{t}}_2$ | 280                   | 1.01                                    | 0.06 : 0.94      | 1.44                                    | 0.89 : 0.11 |
|                                | 320                   | 1.00                                    | 0.04 : 0.96      | 1.45                                    | 0.88 : 0.12 |
|                                | 360                   | 0.98                                    | 0.03 : 0.97      | 1.46                                    | 0.86 : 0.14 |
|                                | 400                   | 0.95                                    | 0.02 : 0.98      | 1.48                                    | 0.85 : 0.15 |

Table 1:  $K$  factors for diagonal stop-pair production at the Tevatron and the LHC for a sample of stop masses. Scale choice:  $\mu = m_{\tilde{t}}$ . The SUGRA-inspired parameters adopted in the calculation of the higher-order corrections are defined in the text. For completeness also the LO initial-state  $gg$  and  $q\bar{q}$  fractions are given.

supersymmetric parameters, *i.e.* the gluino mass, the masses of the light-flavor squarks and the mixing angle. The variation of the cross section with the gluino mass and the mixing angle is indicated by the thick NLO curves. With cross sections typically in the range between 1 and 100 pb, sufficiently large samples of  $10^3$  to  $10^5$  stop events can be accumulated at the Tevatron for an integrated luminosity of  $\int \mathcal{L} = 1 \text{ fb}^{-1}$ , provided these particles exist in the mass range below 200 GeV. For an integrated luminosity of  $\int \mathcal{L} = 100 \text{ fb}^{-1}$  at the LHC a large sample of  $10^5$  to  $10^7$  stop events could be collected for masses in the 200–500 GeV range.

### 3 Mixed $\tilde{t}_1\bar{\tilde{t}}_2$ and $\tilde{t}_2\bar{\tilde{t}}_1$ pairs

In  $p\bar{p}/pp$  collisions, the mixed final states  $\tilde{t}_1\bar{\tilde{t}}_2$  and  $\tilde{t}_2\bar{\tilde{t}}_1$  cannot be produced in lowest order. The production cross section for non-diagonal stop pairs is therefore of order  $\alpha_s^4$ . This higher-order cross section is small but complicated to calculate. We therefore discuss the size of the cross section in the limit of large gluino mass. In this limit, the four-squark couplings relevant for non-diagonal stop-pair production are described by the Lagrangean

$$\mathcal{L}'_4 = \frac{g_s^2}{4} \sin(2\tilde{\theta}) (\tilde{t}_{1i}^* \tilde{t}_{2j} + \tilde{t}_{2i}^* \tilde{t}_{1j}) \left\{ \cos(2\tilde{\theta}) A_2^{ijkl} (\tilde{t}_{1k}^* \tilde{t}_{1l} - \tilde{t}_{2k}^* \tilde{t}_{2l}) + 2 A_1^{ijkl} \sum_{\tilde{q} \neq \tilde{t}} (\tilde{q}_{Lk}^* \tilde{q}_{Ll} - \tilde{q}_{Rk}^* \tilde{q}_{Rl}) \right\} \quad (11)$$

[where however the second term does not contribute to the cross section for mass degenerate left/right light-flavor squarks  $\tilde{q}$ ]. Only two one-loop diagrams contribute to the scattering amplitude in this limit (see Fig. 1c). They involve the production of diagonal  $\tilde{t}_k\bar{\tilde{t}}_k$  pairs in  $gg$  collisions, subsequently transformed to non-diagonal  $\tilde{t}_1\bar{\tilde{t}}_2$  and  $\tilde{t}_2\bar{\tilde{t}}_1$  pairs by rescattering in the final state.

The loops can easily be evaluated:

$$\hat{\sigma}_\infty[gg \rightarrow \tilde{t}_1\bar{\tilde{t}}_2 + \bar{\tilde{t}}_1\tilde{t}_2] = \sin^2(4\tilde{\theta}) \frac{37}{13824} \frac{\alpha_s^4 \lambda^{1/2}}{2\pi s^3} \left| m_{\tilde{t}_1}^2 \log^2(x_1) - m_{\tilde{t}_2}^2 \log^2(x_2) \right|^2 \quad (12)$$

where the subscript in the cross section  $\hat{\sigma}_\infty$  indicates the limit  $m_{\tilde{g}} \rightarrow \infty$ . The coefficient  $\lambda^{1/2}$  is the usual 2-particle phase-space factor, *i.e.*  $\lambda = [s - (m_{\tilde{t}_1} + m_{\tilde{t}_2})^2][s - (m_{\tilde{t}_1} - m_{\tilde{t}_2})^2]/s^2$ , and  $x_k = (\beta_k - 1)/(\beta_k + 1)$ ; the logarithmic singularities are defined properly by the infinitesimal shift  $s \rightarrow s + i\varepsilon$  in  $\beta_k$ .

The cross section depends strongly on the mixing angle  $\tilde{\theta}$  through the overall factor  $\sin^2(4\tilde{\theta})$ . Numerical values for the diagonal and non-diagonal pair cross sections are compared in Table 2 for the default SUGRA-inspired SUSY parameter sets [10] adopted already earlier. Note that the mixed-pair cross section is given in this table *without the mixing factor*  $\sin^2(4\tilde{\theta})$ . Evidently, the values for the cross section for producing mixed stop pairs in the large  $m_{\tilde{g}}$  limit are very small at the Tevatron as well as at the LHC.

|          | $\sigma[\text{fb}]$   | $\sigma_{q\bar{q}}$ | $\sigma_{q\bar{q}}^{\text{limit}}$ | $\sigma_{gg}$     | $\sigma_{gg}^{\text{limit}}$ |
|----------|---|---------------------|------------------------------------|-------------------|------------------------------|
| Tevatron | $\tilde{t}_1\bar{\tilde{t}}_1$                                | $0.64 \cdot 10^3$   | $0.64 \cdot 10^3$                  | $0.42 \cdot 10^3$ | $0.42 \cdot 10^3$            |
|          | $\tilde{t}_2\bar{\tilde{t}}_2$                                | 1.51                | 1.54                               | 0.105             | 0.108                        |
|          | $\tilde{t}_1\bar{\tilde{t}}_2 + \tilde{t}_2\bar{\tilde{t}}_1$ | –                   | 0                                  | –                 | $1.54 \cdot 10^{-4}$         |
| LHC      | $\tilde{t}_1\bar{\tilde{t}}_1$                                | $0.60 \cdot 10^3$   | $0.59 \cdot 10^3$                  | $6.50 \cdot 10^3$ | $6.47 \cdot 10^3$            |
|          | $\tilde{t}_2\bar{\tilde{t}}_2$                                | 37.1                | 37.1                               | $0.23 \cdot 10^3$ | $0.24 \cdot 10^3$            |
|          | $\tilde{t}_1\bar{\tilde{t}}_2 + \tilde{t}_2\bar{\tilde{t}}_1$ | –                   | 0                                  | –                 | $3.53 \cdot 10^{-2}$         |

Table 2: *Cross sections for diagonal and non-diagonal pair production at the Tevatron and the LHC, using the default SUGRA-inspired values for the SUSY parameters. The non-diagonal results are given without the mixing factor  $\sin^2(4\tilde{\theta})$ . Scale choice: average mass of the produced stop particles. The superscript 'limit' denotes the asymptotic value of the cross section for large gluino masses.*

## 4 Summary

The picture that has emerged from the SUSY-QCD analysis, is quite simple. (i) The cross sections for the production of diagonal pairs  $p\bar{p}/pp \rightarrow \tilde{t}_1\bar{\tilde{t}}_1, \tilde{t}_2\bar{\tilde{t}}_2$  depend essentially only on the masses of the stop particles produced and very little on the other supersymmetric parameters. Bounds on the  $\tilde{t}_1\bar{\tilde{t}}_1$  production cross section can therefore easily be translated into lower bounds on the lightest stop mass without reference to other supersymmetric parameters. On the other hand, if stop particles were to be discovered, the cross section can be exploited directly to determine the two stop masses  $m_{\tilde{t}_1}$  and  $m_{\tilde{t}_2}$ . (ii) If mixed stop pairs could be discovered in  $pp \rightarrow \tilde{t}_1\bar{\tilde{t}}_2 + \tilde{t}_2\bar{\tilde{t}}_1$  for sufficiently high integrated luminosity, the mixing angle can be derived



from the magnitude of the cross section which is proportional to  $\sin^2(4\tilde{\theta})$ . In contrast to mixed stop-pair production via  $Z$  exchange in  $e^+e^-$  annihilation [11], the cross section is suppressed by  $\mathcal{O}(\alpha_s^2)$  with respect to diagonal pair production.

**Acknowledgements:** We are very grateful to S. Lammel for advise and discussions on the search for stop particles at the Tevatron. Collaboration with R. Höpker is also gratefully acknowledged. W.B., M.K. and M.S. thank the DESY Theory Group for the warm hospitality extended to them during a visit.

**Note:** The program for calculating the stop cross sections has been included into the package PROSPINO, <http://wwwcn.cern.ch/~mspira>.

## References

- [1] J. Ellis and S. Rudaz, *Phys. Lett.* **B128** (1983) 248.
- [2] See e.g. A. Djouadi, J. Kalinowski, P. Ohmann, and P.M. Zerwas, *Z. Phys.* **C74** (1997) 93; V. Barger, M.S. Berger, and P. Ohmann, *Phys. Rev.* **D47** (1993) 1093 and *Phys. Rev.* **D49** (1994) 4908.
- [3] K. Ackerstaff *et al.*, Opal Collaboration, *Z. Phys.* **C75** (1997) 409; R. Barate *et al.*, Aleph Collaboration, CERN-PPE/97-084 [*hep-ex/9708013*].
- [4] S. Abachi *et al.*, D0 Collaboration, *Phys. Rev. Lett.* **76** (1996) 2222.
- [5] G.L. Kane and J.P. Leveille, *Phys. Lett.* **B112** (1982) 227; P.R. Harrison and C.H. Llewellyn Smith, *Nucl. Phys.* **B213** (1983) 223 and Erratum *ibid.*; E. Reya and D.P. Roy, *Phys. Rev.* **D32** (1985) 645; S. Dawson, E. Eichten and C. Quigg, *Phys. Rev.* **D31** (1985) 1581; H. Baer and X. Tata, *Phys. Lett.* **B160** (1985) 159.
- [6] W. Beenakker, R. Höpker, M. Spira, and P.M. Zerwas, *Phys. Rev. Lett.* **74** (1995) 2905, *Z. Phys.* **C69** (1995) 163 and *Nucl. Phys.* **B492** (1997) 51; W. Beenakker, R. Höpker, and M. Spira, *hep-ph/9611232*.
- [7] W. Beenakker, R. Höpker, T. Plehn, and P.M. Zerwas, *Z. Phys.* **C75** (1997) 349; A. Djouadi, W. Hollik, and C. Jünger, *Phys. Rev.* **D55** (1997) 6975; S. Kraml, H. Eberl, A. Bartl, W. Majerotto, and W. Porod, *Phys. Lett.* **B386** (1996) 175; for a general analysis of the mixing formalism see also M.A. Diaz, Proceedings, Meeting of the American Physical Society, Albuquerque, DPF Conf. 1994.
- [8] S.P. Martin and M.T. Vaughn, *Phys. Lett.* **B318** (1993) 331.
- [9] H.L. Lai *et al.*, *Phys. Rev.* **D55** (1997) 1280.
- [10] M. Drees and S.P. Martin, Madison report MAD-PH-879 [*hep-ph/9504324*]; S. Mrenna, *Comp. Phys. Commun.* **101** (1997) 232.

- [11] A. Bartl, H. Eberl, S. Kraml, W. Majerotto, W. Porod, and A. Sopczak, in ‘ $e^+e^-$  Collisions at TeV Energies: The Physics Potential’, ed. P.M. Zerwas, DESY 96-123D; see also E. Accomando *et al.*, ‘Physics with  $e^+e^-$  Linear Colliders’, DESY 97-100 and hep-ph/9705442 (*Phys. Rep. C* in press).

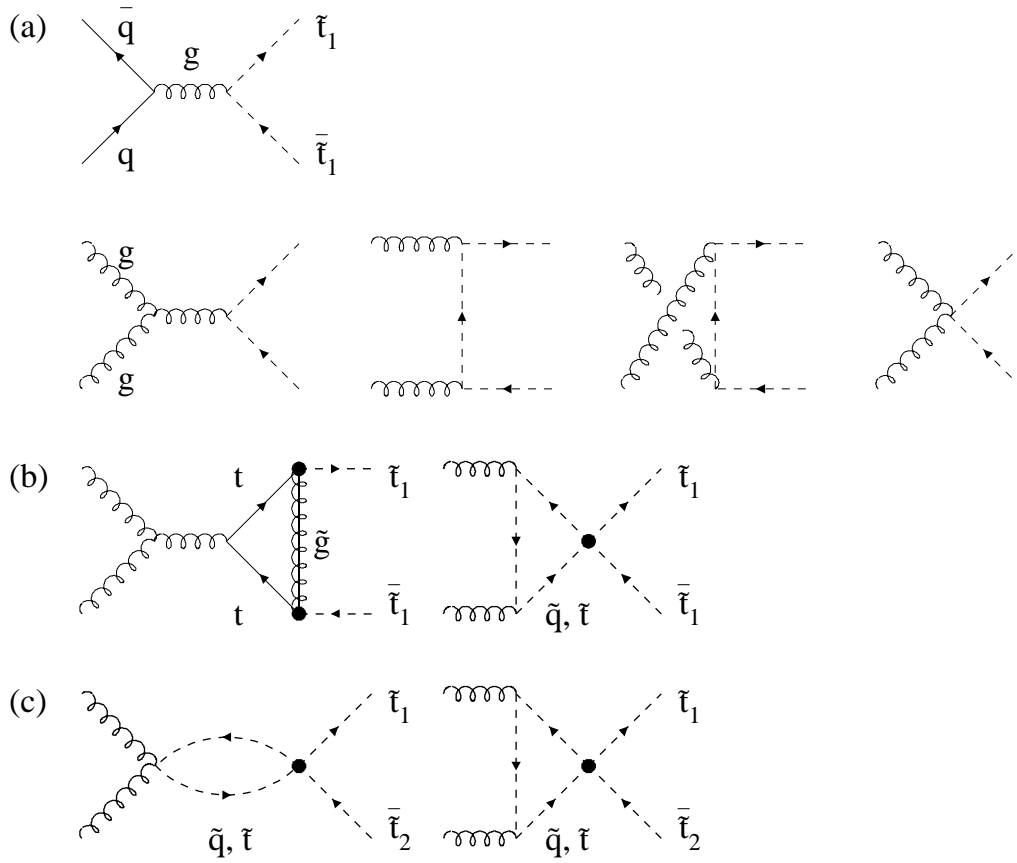


Figure 1: *Generic Feynman diagrams for the production of pairs of stop particles: (a) Born diagrams for quark-antiquark annihilation and gluon fusion; (b) higher-order diagrams for the diagonal production including stop mixing (dotted vertices); (c) non-diagonal production in the limit of decoupled gluinos (mixing vertices are dotted).*

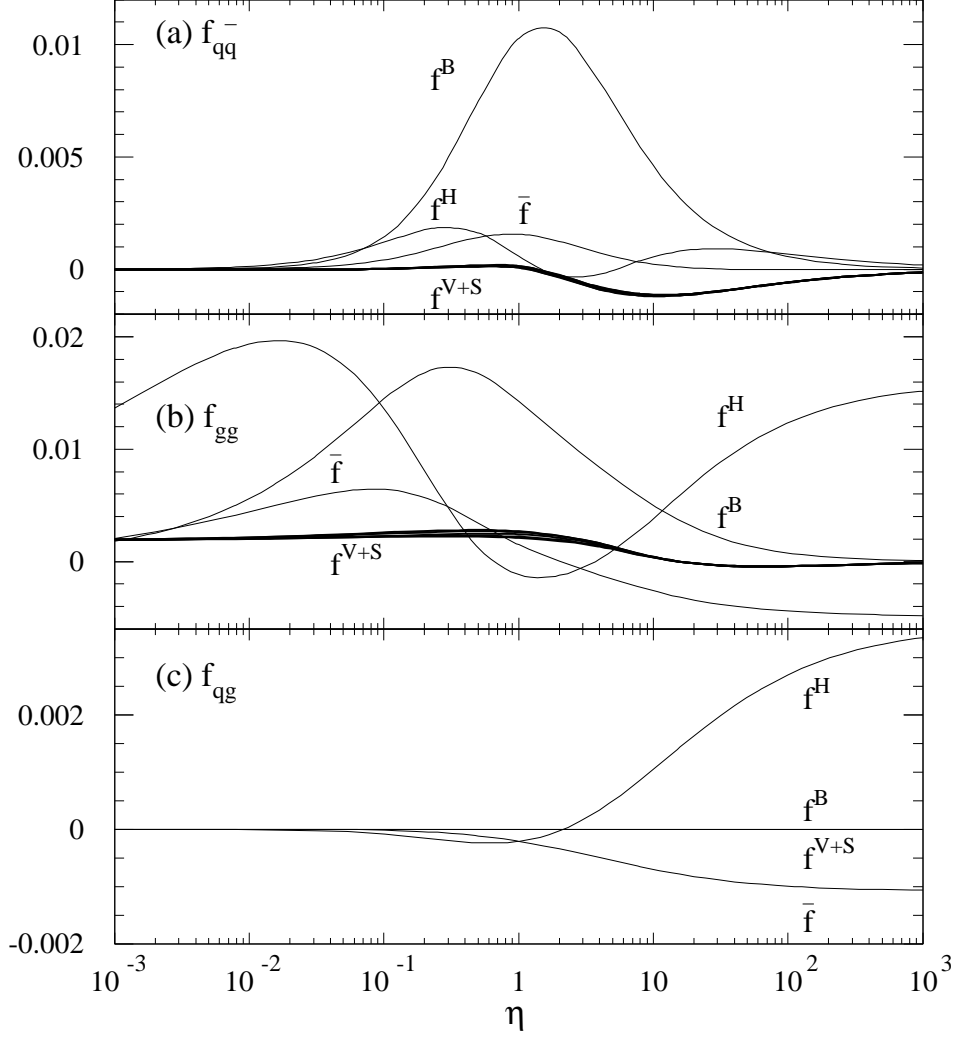


Figure 2: The scaling functions for the production of  $\tilde{t}_1\tilde{t}_1^*$  pairs as a function of  $\eta = s/4m_{\tilde{t}_1}^2 - 1$ . The notation follows Eq. (8). The variation of the scaling function  $f_{ij}^{V+S}$  for all possible values of the mixing angle  $\tilde{\theta}$  is indicated by the line-thickness of the corresponding curves. The scaling functions  $f_{g\bar{q}}$  are identical to  $f_{qg}$ .

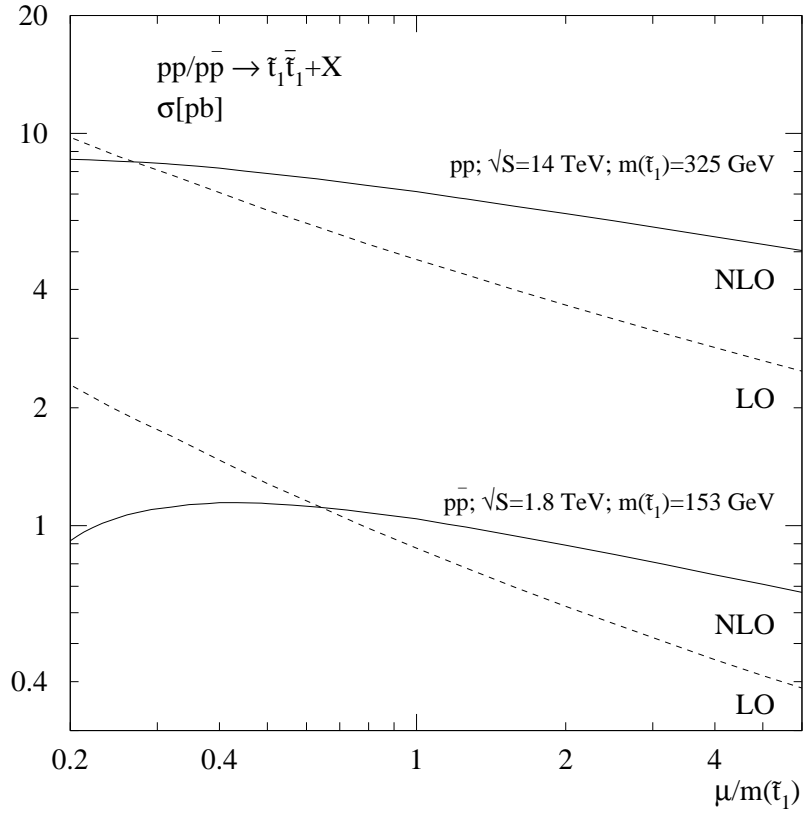


Figure 3: Renormalization/factorization-scale dependence of the total cross sections for  $\tilde{t}_1$ -pair production at the Tevatron and the LHC. The SUSY mass parameters correspond to the central values of the SUGRA-inspired scenario described in the text.

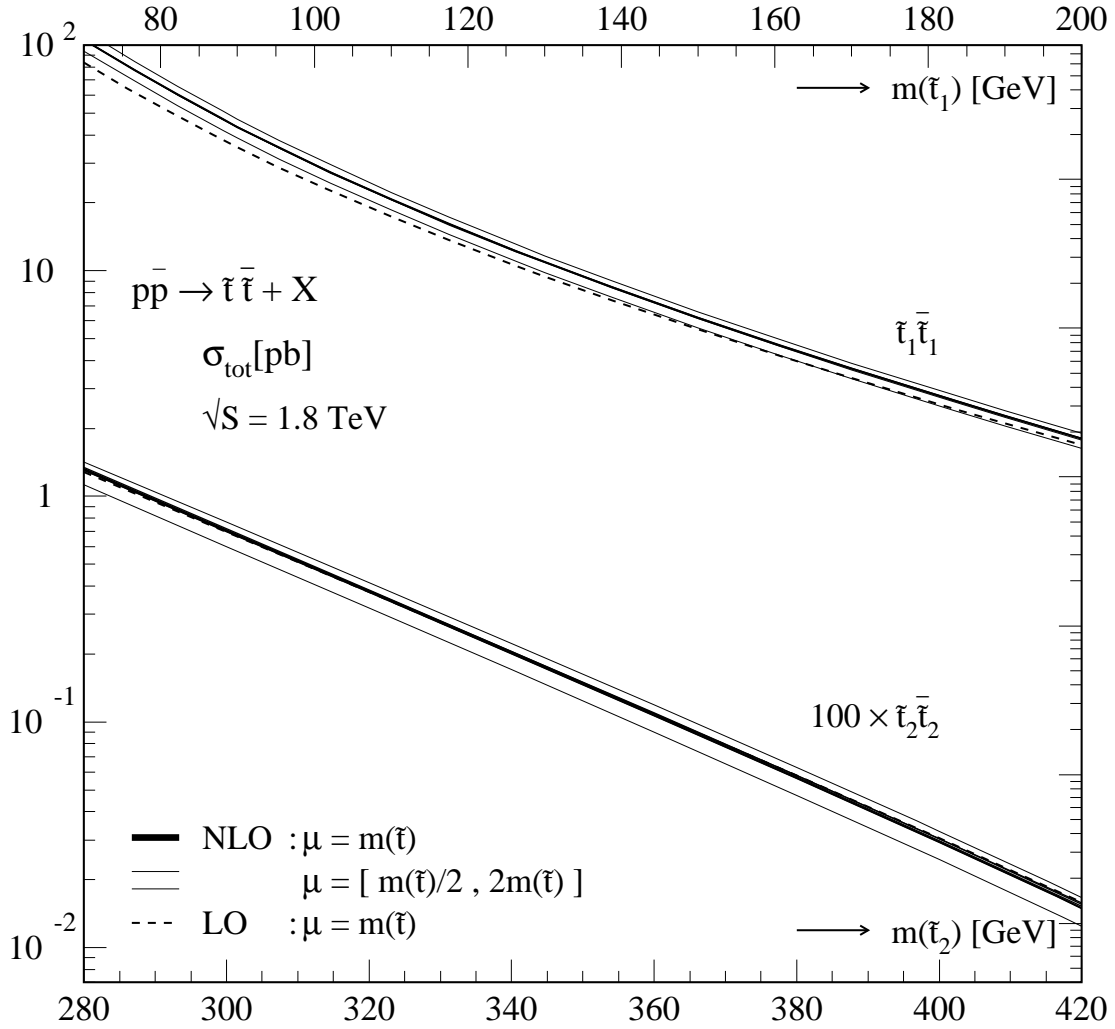


Figure 4: The total cross sections for the production of pairs of stop particles ( $\tilde{t}_k\tilde{t}_k$ ) at the Tevatron as a function of the stop masses. The band for the NLO result indicates the uncertainty due to the renormalization/factorization scale. The light-flavor squark masses, the gluino mass and the mixing parameter are derived within the SUGRA-inspired scenario defined in the text. The line-thickness of the NLO curves represents the simultaneous variation of the gluino mass between 200 (284) and 800 GeV for  $\tilde{t}_1(\tilde{t}_2)$ -pair production and the variation of  $\sin(2\theta)$  over its full range.

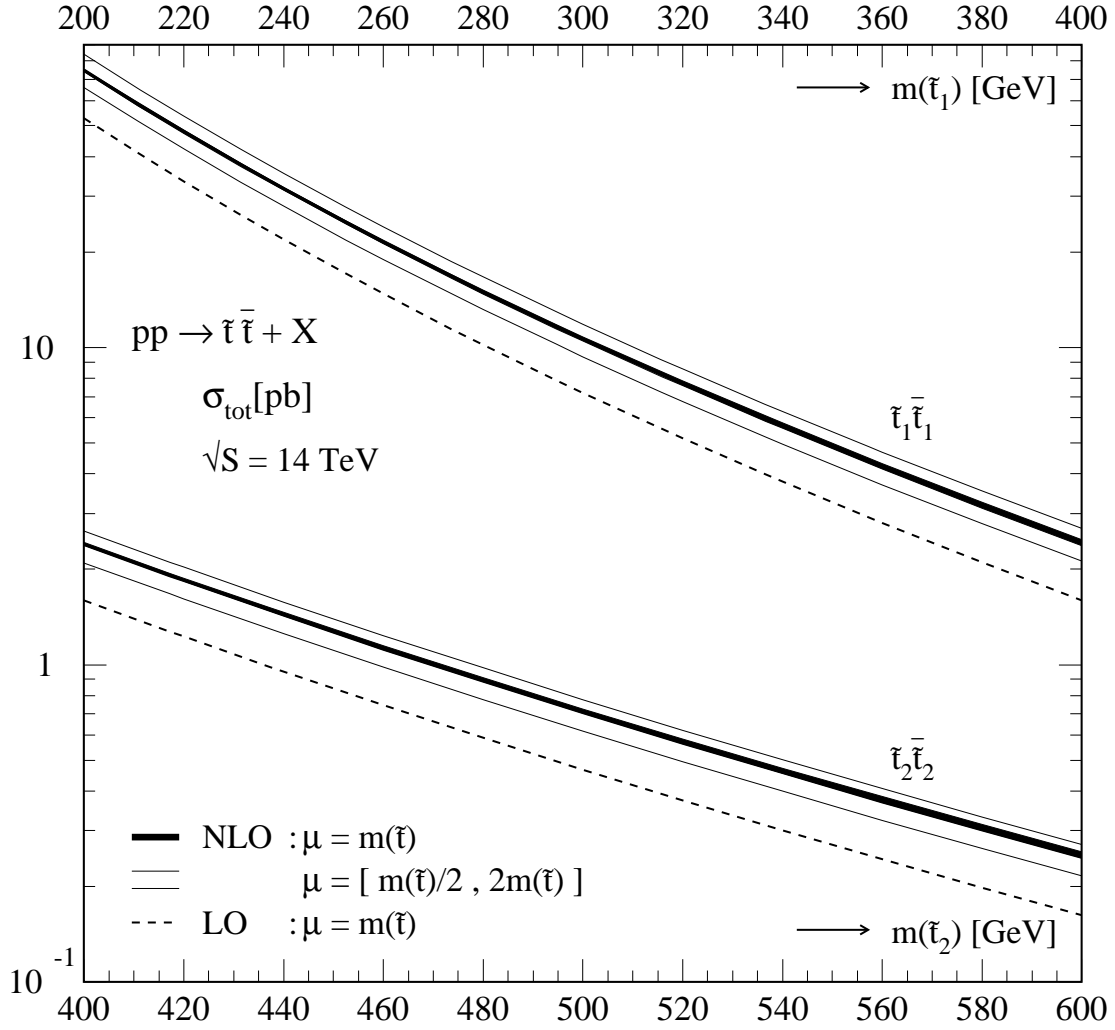


Figure 5: The same as Fig. 4, but for the LHC. The SUSY mass spectrum is described in the text. The gluino mass is varied between 400 (600) and 900 GeV for  $\tilde{\tau}_1(\tilde{\tau}_2)$ -pair production.